Available online at www.sciencedirect.com
SCIENCE @ DIRECT®
Geomorphology 53 (2002) 165–181
GEOMORPHOLOGY
www.elsevier.com/locate/geomorph

Ground penetrating radar: 2-D and 3-D subsurface imaging of a coastal barrier spit, Long Beach, WA, USA

Harry M. Jol[a,*], Don C. Lawton[b], Derald G. Smith[c]

[a] *Department of Geography, University of Wisconsin-Eau Claire, 105 Garfield Avenue, Eau Claire, WI 54702-4004, USA*
[b] *Department of Geology and Geophysics, University of Calgary, 2500 University Avenue, Calgary, AB, Canada T2N 1N4*
[c] *Department of Geography, University of Calgary, 2500 University Avenue, Calgary, AB, Canada T2N 1N4*

Received 28 August 2001; received in revised form 15 July 2002; accepted 1 August 2002

Abstract

The ability to effectively interpret and reconstruct geomorphic environments has been significantly aided by the subsurface imaging capabilities of ground penetrating radar (GPR). The GPR method, which is based on the propagation and reflection of pulsed high frequency electromagnetic energy, provides high resolution (cm to m scale) and shallow subsurface (0–60 m), near continuous profiles of many coarser-grained deposits (sediments of low electrical conductivity). This paper presents 2-D and 3-D GPR results from an experiment on a regressive modern barrier spit at Willapa Bay, WA, USA. The medium-grained sand spit is 38 km long, up to 2–3.5 km wide, and is influenced by a 3.7-m tidal range (spring) as well as high energy longshore transport and high wave energy depositional processes. The spit has a freshwater aquifer recharged by rainfall.

The GPR acquisition system used for the test was a portable, digital pulseEKKO™ system with antennae frequency ranging from 25 to 200 MHz and transmitter voltages ranging from 400 to 1000 V. Step sizes and antennae separation varied depending on the test requirements. In addition, 100-MHz antennae were used for conducting antennae orientation tests and collecting a detailed grid of data (50 × 50 m sampled every meter). The 2-D digital profiles were processed and plotted using pulseEKKO™ software. The 3-D datasets, after initial processing, were entered into a LANDMARK™ workstation that allowed for unique 3-D perspectives of the subsurface. To provide depth, near-surface velocity measurements were calculated from common midpoint (CMP) surveys.

Results from the present study demonstrate higher resolution from the 200-MHz antennae for the top 5–6 m, whereas the 25- and 50-MHz antennae show deeper penetration to >10 m. For the study site, 100-MHz antennae provided acceptable resolution, continuity of reflections, and penetration. The dip profiles show a shingle-like accretionary depositional pattern, whereas strike profiles show a horizontal and subhorizontal, nearly continuous reflection pattern. Results from the GPR experiment reveal upper shoreface reflections with dip towards the ocean at about 1–2°. The loss of signal from below a depth of 6–8 m indicates a lithofacies change because of the storm wave base.

The parallel broadside and perpendicular broadside antennae orientation tests show detailed stratigraphy, continuity, and depth of penetration. The cross-polarization test exhibits reduced continuity of reflections and less depth of penetration, but dipping reflections are apparent.

The grid pattern data provided a detailed view of 3-D geometry of individual reflections. High quality data were obtained, processed, and directly exported into a LANDMARK™ workstation for interpretation. The resulting interpretations of the upper shoreface beds from the test cube (50 × 50 m; total 2600 traces) are shown as vertical sections (slices), horizontal sections (time

* Corresponding author. Tel.: +1-715-836-3472; fax: +1-715-836-6027.
E-mail address: jolhm@uwec.edu (H.M. Jol).

doi: 10.1016/S0169-555X(02)00352-5

slices), contour maps, 3-D representations of individual beds, and an isopach map. The 3-D depositional framework allows a more detailed interpretation than widely spaced 2-D profiles.

Keywords: Coastal; Ground penetrating radar; Barrier; Spits; Washington

1. Introduction

Barrier spits are narrow, elongated bodies of coarse-grained sediments (e.g., sand or gravel) that form when sediment is transported and deposited by longshore drift and wave processes. North American examples can be found along most of the U.S. Atlantic coast, and Gulf of Mexico, with isolated segments along the Pacific coast, Gulf of St. Lawrence, and Arctic coast. Many of the modern barrier systems are becoming heavily populated because of their desirable locations. Often, little geological or environmental planning is conducted prior to human development. This can lead to freshwater aquifers becoming depleted by overuse and/or becoming brackish, leading to a loss of local drinking water. In addition, an increase in the number of septic/garbage fields affects the quality of the freshwater aquifer. A better understanding of barrier-spit depositional systems is needed to assist informed decision-making during the planning stages of developments and for remediation of already affected coastal communities.

Barrier depositional systems in the subsurface have also been the site for many significant oil and gas discoveries over the last several decades (Chiang, 1984; Smith et al., 1984). A resurgence of geologic interest in barriers as targets for oil and gas exploration has lead to increased research, hence knowledge of their internal geometries is important for oil field development. As well, an evolving awareness exists that many of the ancient barriers were deposited in an environment influenced by high wave energy with a 2- to 4-m tide range (mesotidal). These ancient depositional settings were probably different than the lower tidal and wave energy conditions of the present-day Atlantic and Gulf coasts of the U.S. from where most of the depositional models have been generated (Reinson, 1984). The Long Beach coastal setting of Washington State is influenced by a higher (3.7 m) tidal range and by high wave energy depositional processes, quite different than areas discussed along the Atlantic and Gulf coasts.

The ability to effectively interpret and reconstruct these coastal geomorphic environments has been significantly aided by ground penetrating radar's (GPR) subsurface imaging capabilities (e.g., Leatherman, 1987; Jol and Smith, 1991; Bristow, 1995; Jol et al., 1996b; Van Heteren et al., 1996, 1998; Neal and Roberts, 2000). The GPR method, which is based on the propagation and reflection of pulsed high frequency electromagnetic energy, provides high resolution (cm to m scale), shallow subsurface (0–60 m), near continuous profiles of many coarser-grained deposits (sediments of low electrical conductivity). The objectives of the study at a test site on the Willapa barrier spit are (i) to collect and assess the two- and three-dimensional (2-D; 3-D) GPR datasets generated at a test site on the Willapa barrier spit; (ii) to compare the GPR reflection patterns for different antennae frequencies (25, 50, 100, and 200 MHz), different transmitter powers (400 and 1000 V), and different antennae orientations; and (iii) to determine whether GPR can be used to map the 3-D subsurface geometry of a marine barrier system.

2. Site description

The field site in coastal Washington State, USA, is part of a modern, active 38-km-long by 2- to 3.5-km-wide barrier spit (Fig. 1). The barrier, located at Willapa Bay north of the Columbia River mouth, is one of the most prominent along the west coast of North America. It is composed of medium-grained, well-sorted beach sand, which is influenced by a 3.7-m tidal range (spring) and high energy wave and longshore transport system (Clifton, 1983). The water table in the study area is within 2 m of the surface. The surface of the barrier is covered with eolian dune ridges (up to 7 m thick) and peat bogs, which were deposited over time as the beach accreted towards the

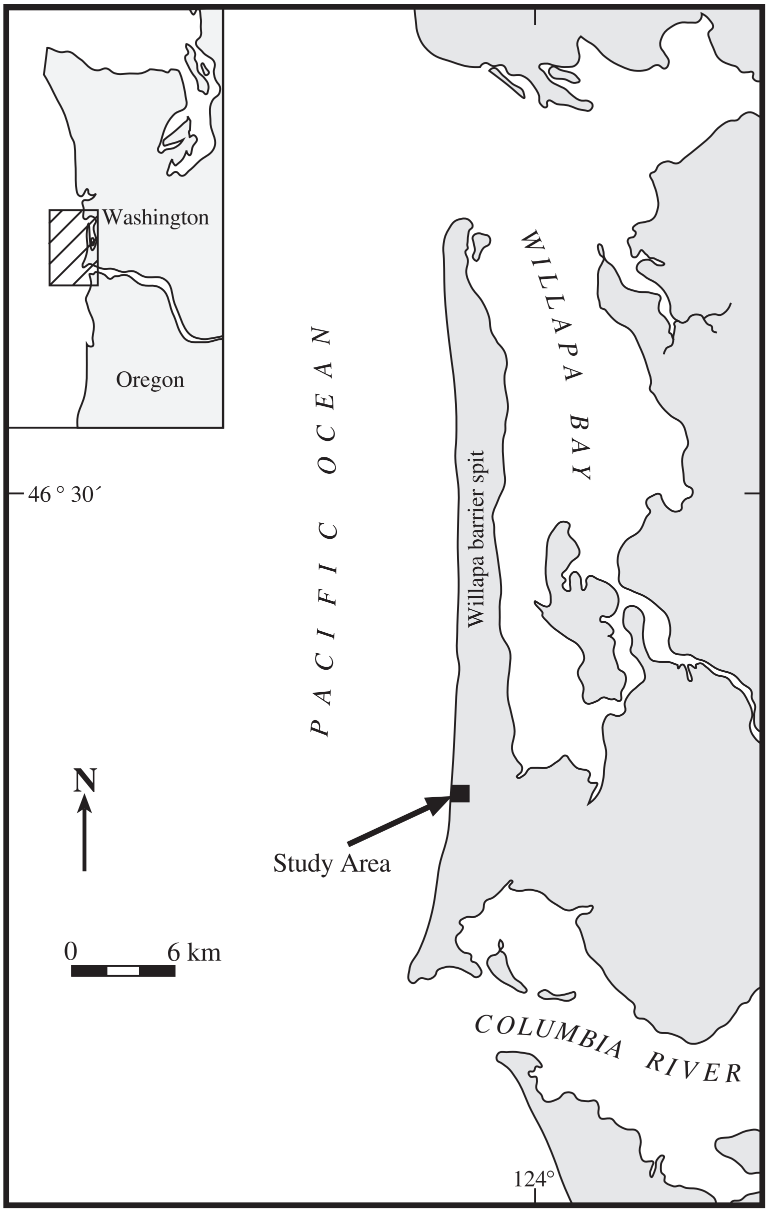

Fig. 1. Location map of Willapa Bay and coastal barrier spit. Box identifies study site located immediately north of the access road to Nendels Edgewater Inn (see Figs. 2–4; modified from Clifton and Phillips, 1980).

ocean. A library search of old maps and photographs showing shoreline positions, as well as discussions with local residents of Long Beach, revealed that the barrier at the test site location has prograded several hundred meters over the past 80 years (Figs. 2 and 3).

The barrier has an internal freshwater aquifer recharged by rainfall (~ 2.0 m/year) that, combined with the clean beach and aeolian sand, allowed for exceptionally high quality GPR results. Previous GPR tests indicated a favorable environment to un-

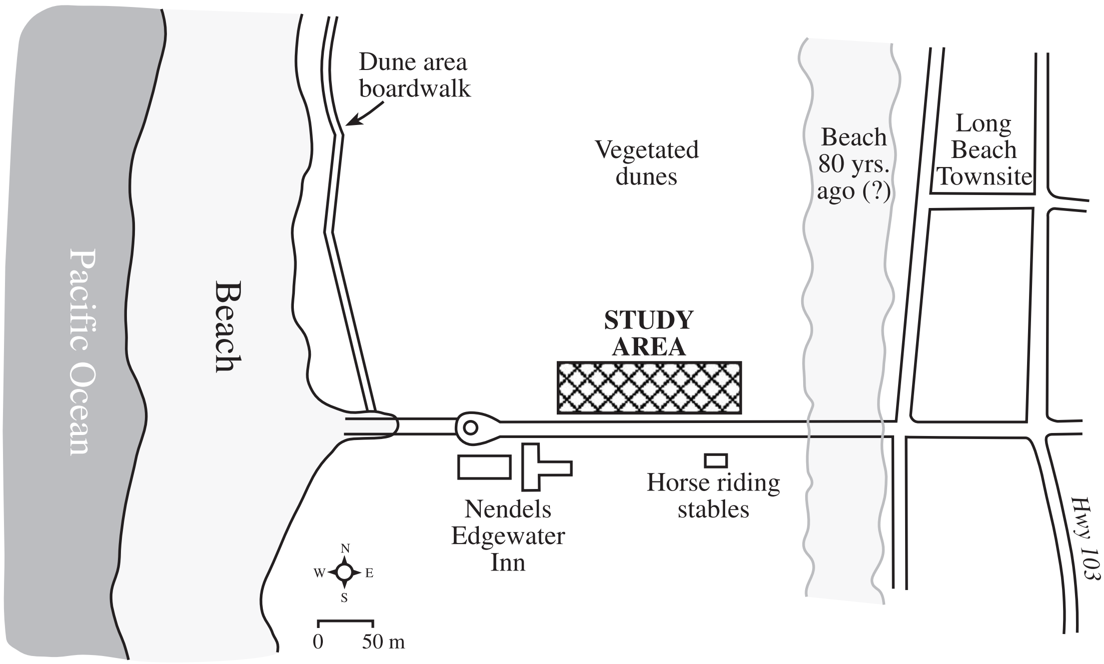

Fig. 2. Location of study area. The test site is ~ 200 m west of the Long Beach town site and 300 m inland (east) of the high tide line.

dertake a more intensive GPR program (Meyers, 1994; Jol et al., 1996a,b; Meyers et al., 1996; Smith et al., 1999).

The test site is part of a larger study undertaken to investigate modern analogues to ancient hydrocarbon reservoirs (Smith et al., 1999) as well as

Fig. 3. Oblique aerial photo of the study area is taken from the west showing the open field where the GPR tests were conducted.

part of a regional study of sediment dynamics in the Columbia River littoral cell (Southwest Washington Coastal Erosion Program; Kaminsky et al., 1999).

The test site is located ~200 m west of the Long Beach town site and ~300 m inland from the high tide line of the Pacific Ocean (Figs. 2 and 3). The sandy site had been leveled several years previously and recently mowed. The clearing measures ~160 × 57 m. It is bordered on the south by a paved beach access road and in all other directions by vegetated beach dunes. Fig. 4 provides a schematic layout of the GPR profiles and survey area.

The field research was carried out during the summer months, which are regarded as the best time period for optimum weather conditions in the area. Also during these months, following the winter and spring rainy season, the beach sediments contain a high percentage of freshwater. This is an important requirement because the GPR method has severe signal loss problems in saline and brackish ground water conditions, which occurred at ~100 m landward of the high tide line.

3. Methodology

Subsurface profiling with GPR is similar to seismic reflection, the difference being that GPR uses electromagnetic (EM) energy rather than acoustic energy. A short pulse of high frequency EM energy, usually in the 10- to 1000-MHz range, is transmitted into the ground generating a wavefront that propagates downward. Because of a change in the bulk electrical properties of different subsurface lithologies, mineralogy, and/or the character of the sediment interface, some of the energy is reflected back to the surface (Davis and Annan, 1989). At the surface, a receiver monitors reflected energy versus delay time. The pulse delay time from the energy transmitted into the ground and reflected back to the receiver is a function of the EM propagation velocity through the sediment and the depth of subsurface reflectors. Strength of the reflected signal is approximately proportional to the difference in dielectric constants at the sediment interface (Davis and Annan, 1989). These effects enable the subsurface stratigraphy and structure to be inferred from the character of the radar

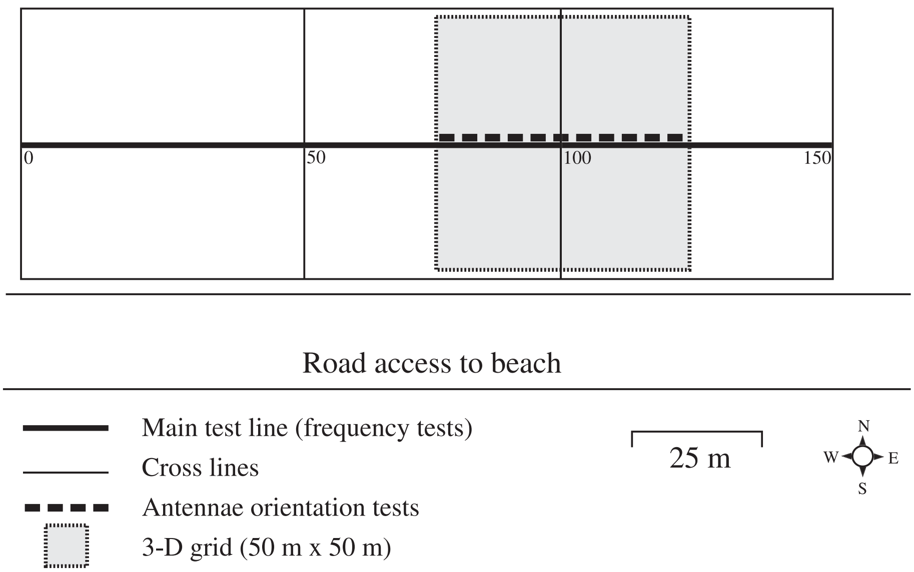

Fig. 4. Details of the test site. The test site is ~150 m long and 57 m wide, consisting of cleared and leveled land. The main test line (150 m; west to east) runs down the axis of the test site. The 25-, 50-, 100-, and 200-MHz antennae and transmitter voltage comparisons were along this line. The crosslines run perpendicular to the main line at 50 and 100 m. The antennae orientation tests were run from 100 to 125 m on the main line, while the 50 × 50 m grid was centered on the 100-m point of the main line.

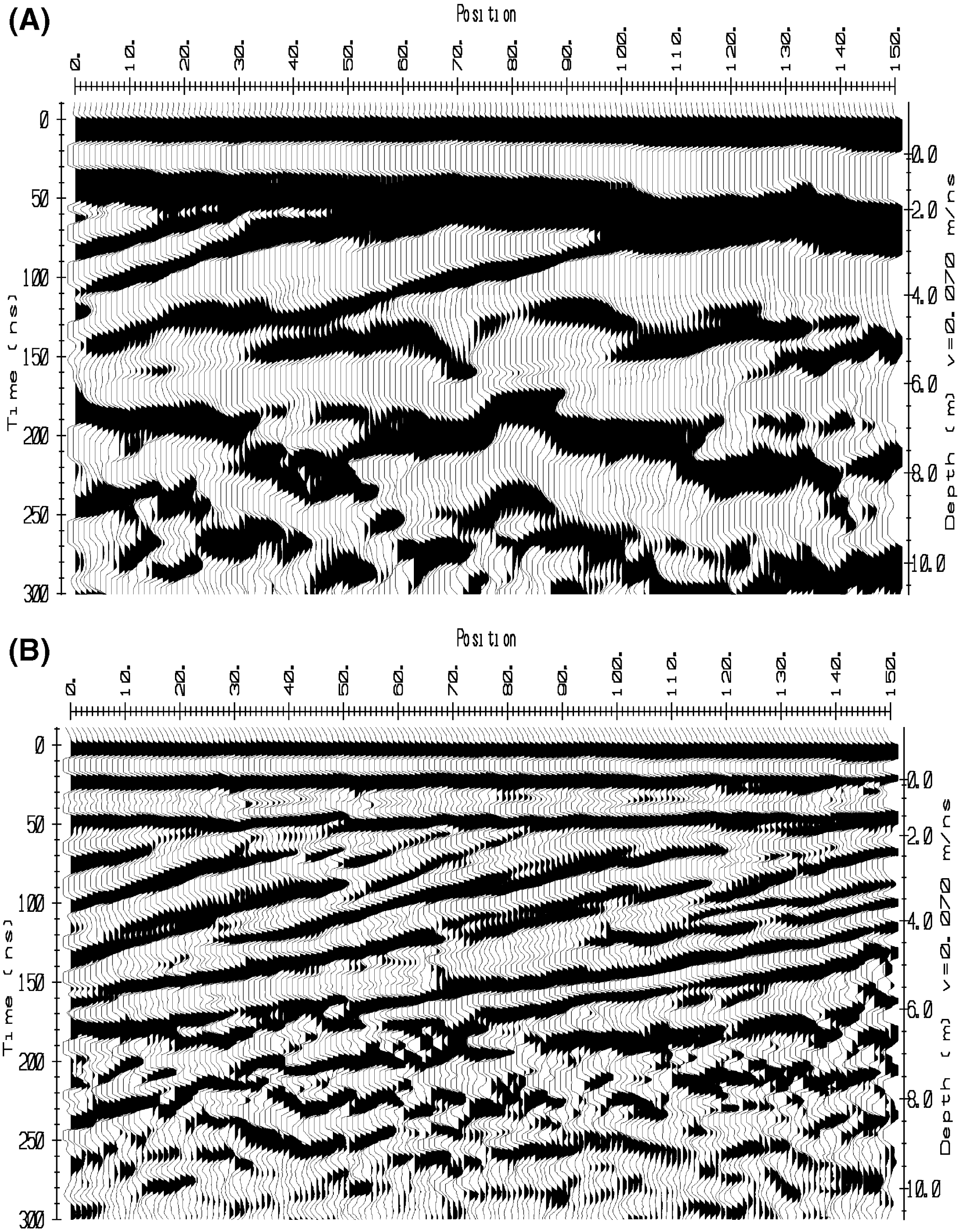

Fig. 5. Comparison of antennae frequencies with 1000-V transmitter along the main test line (*x*-axis—distance in meters, 1-m trace interval; see Fig. 4 for location; 0 m—west, 150 m—east). Inclined reflections represent beachface depositional strata. There appears to be a lithofacies change at a depth of 6 m. (A) 25 MHz/1000 V transmitter; (B) 50 MHz/1000 V transmitter; (C) 100 MHz/1000 V transmitter; (D) 200 MHz/1000 V transmitter.

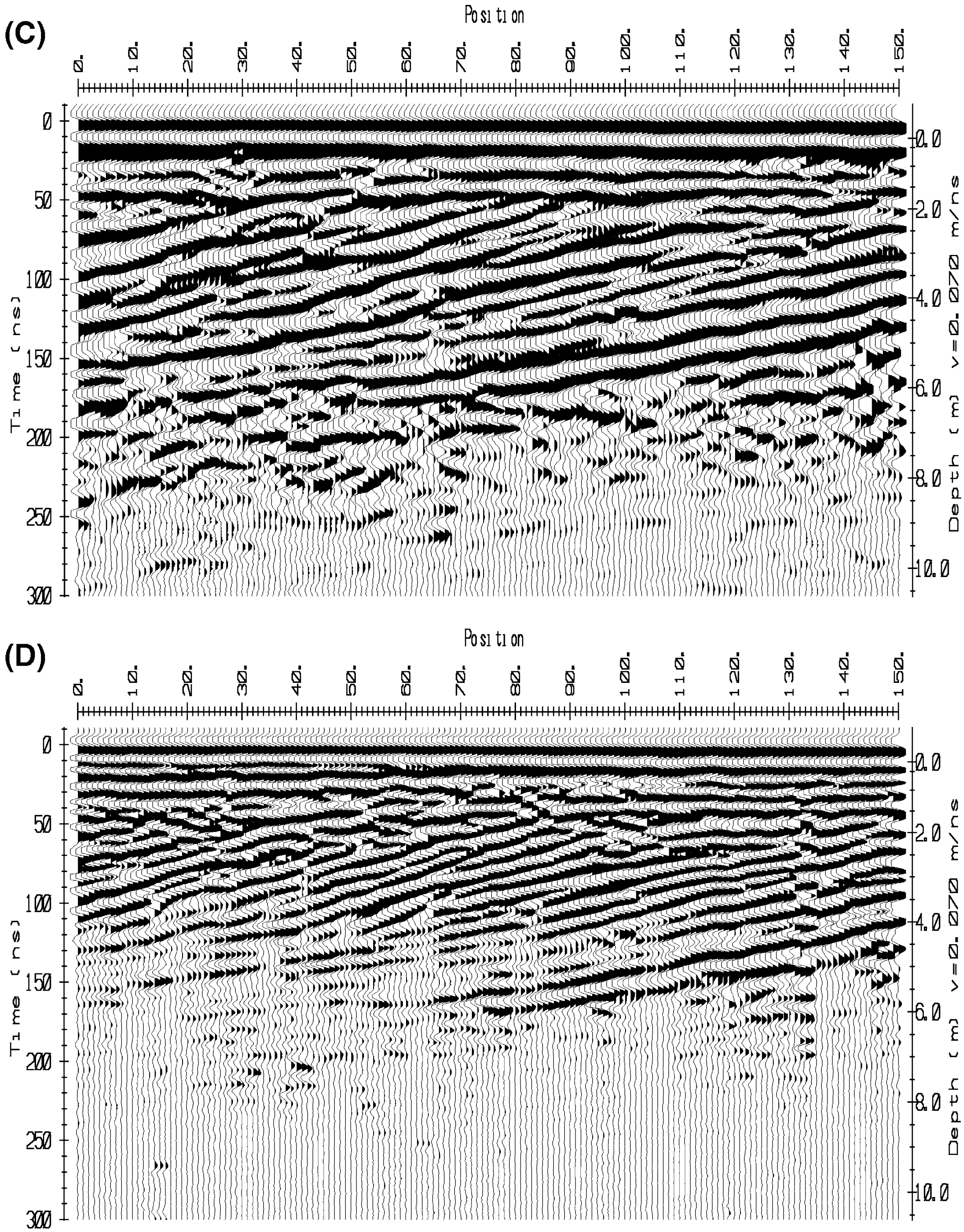

Fig. 5 (*continued*).

return signals. Changes in the dielectric constant and electrical conductivity can also affect the rate of energy attenuation. Because fine-grained sediments such as silts and clays (which have high conductivities) cause high signal attenuation and reduce the penetration depth to a few meters or less, GPR is limited to environments of low conductivity. GPR provides a profile of horizontal survey distance (m) versus vertical two-way travel time in nanoseconds ($1\ ns = 10^{-9}\ s$). By measuring the propagation velocity of sediment, depth of reflections can be determined. Further GPR theory and methodology are adequately explained elsewhere (Ulriksen, 1982; Daniels et al., 1988; Davis and Annan, 1989; Jol and Smith, 1991).

A portable, digital, pulseEKKO™ radar system was used in the reflection survey mode to obtain the

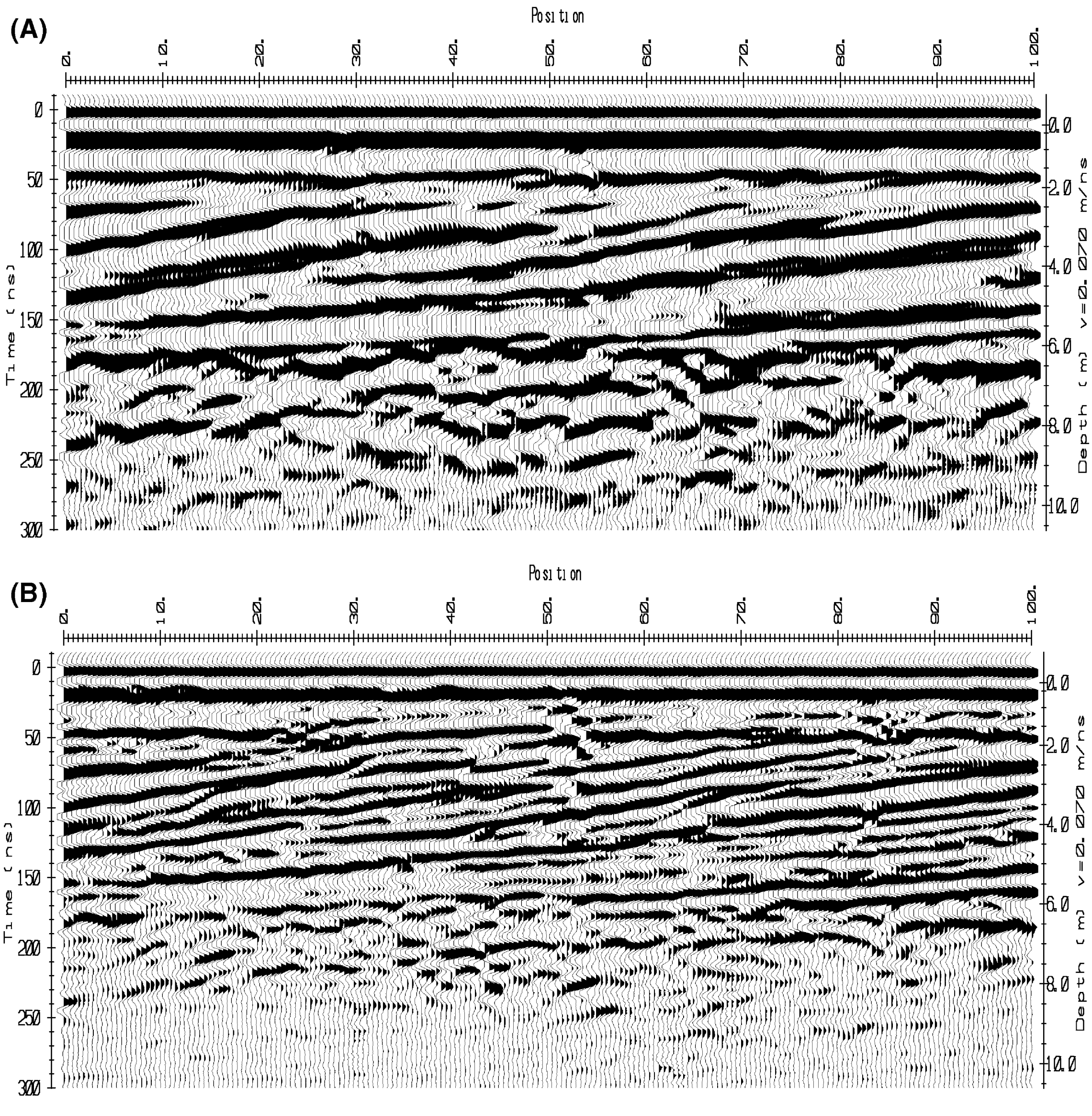

Fig. 6. Comparison of antennae frequencies with 400 V transmitter along the main test line (*x*-axis—distance in meters, 0.5-m trace interval; see Fig. 4 for location; 0 m—west, 150 m—east). (A) 50 MHz/400 V transmitter; (B) 100 MHz/400 V transmitter; (C) 200 MHz/400 V transmitter.

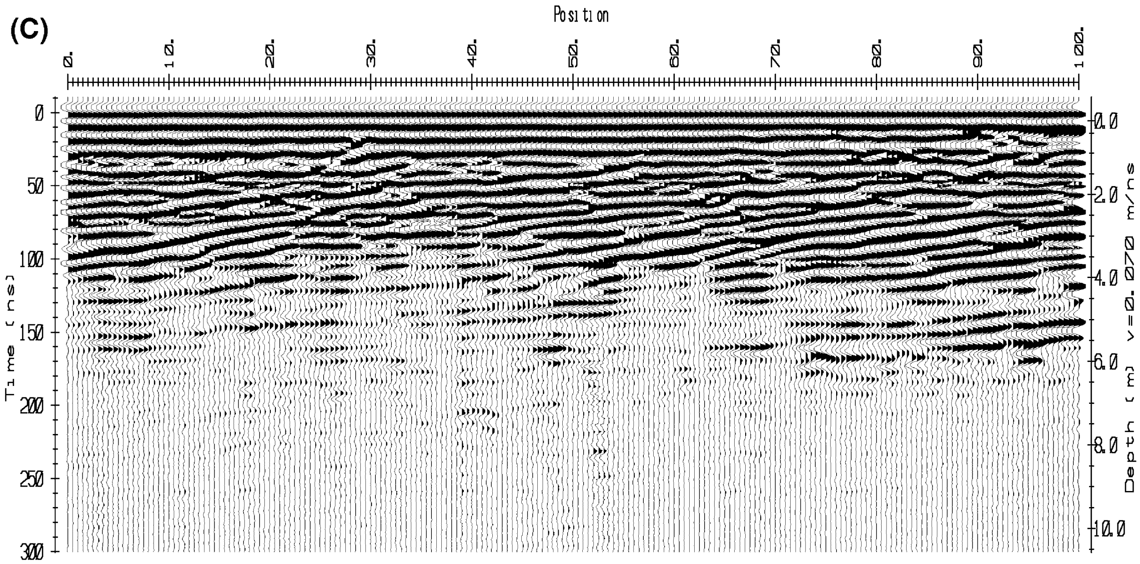

Fig. 6 (*continued*).

GPR profiles. This robust system allows the operator to obtain digital recordings of time series traces for radar amplitude at discrete locations within the survey area. Antennae frequencies of 25, 50, 100, and 200 MHz were tested using transmitters with two different voltages (400 and 1000 V). Traces at each surface location were digitized at a sampling time interval of 800 picoseconds (1 ps $=10^{-12}$ s) and vertically stacked 64 times. The digital profiles were processed and plotted (wiggle trace format) using pulseEKKO™ software with automatic gain control (AGC), signal saturation correction, trace stacking (horizontal averaging), and point stacking (running average). Further processing was conducted on several of the profiles. All stated dip angles have been corrected to include migration. An average, near-surface velocity of 0.07 m/ns was determined from common midpoint (CMP) surveys conducted at the site.

Vibracoring of the barrier sediments was very difficult as a result of the high degree of compaction and sorting of sand by wave energy.

4. Results and interpretation

For the sake of clarity, the horizontal scale of all profiles is distance in meters, whereas the vertical scale is shown as both two-way travel time (ns; left side) and depth in meters (m; right side) based on the near-surface velocity of a radar pulse through the sediment. The two uppermost continuous reflections in all profiles represent air wave and ground wave arrivals, respectively, and should not be considered part of the stratigraphic data.

4.1. Comparison of antennae frequency and voltage power

At any study site, the requirements for depth of penetration, resolution, and continuity of reflections should be considered before antennae frequency and transmitter pulser voltage are selected (Davis and Annan, 1989; Jol, 1995; Smith and Jol, 1995). Changing the center frequency of the GPR antennae permits selective enhancement of the subsurface responses at different scales. GPR systems allow for a range of antennae frequency and transmitter powers to be exploited. The pulseEKKO™ system unit can be used with antennae frequencies of 12.5, 25, 50, 100, and 200 MHz, as well as transmitter voltages of 400 and 1000 V.

A comparison of GPR results along the main test line for different antennae frequencies from the Long Beach study site are shown in Figs. 5 and 6. They

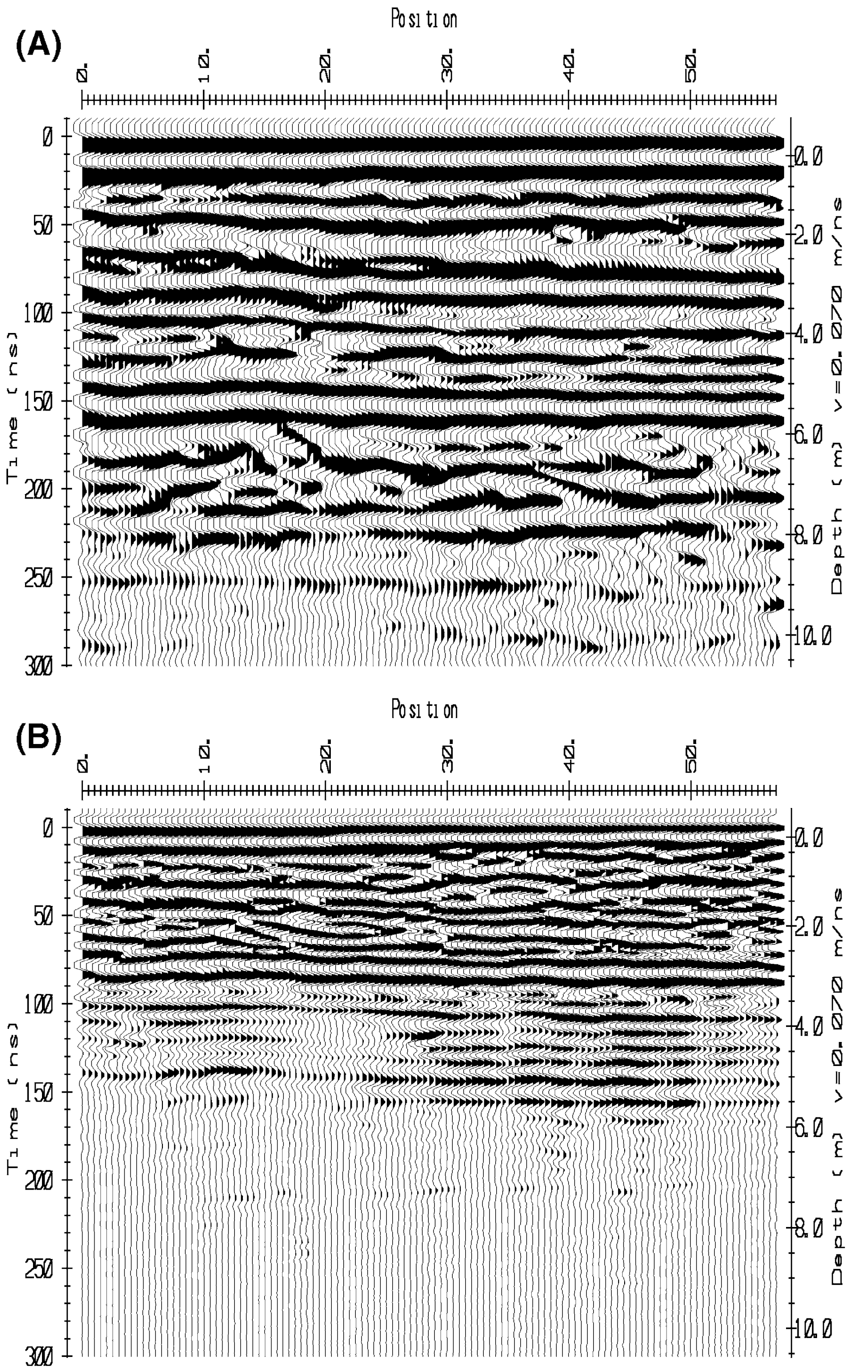

Fig. 7. Crossline at 100 m of main test line (*x*-axis—distance in meters, 0.5-m trace interval; 0 m—south, 60 m—north; see Fig. 4 for location). (A) 100 MHz/1000 V; (B) 200 MHz/400 V.

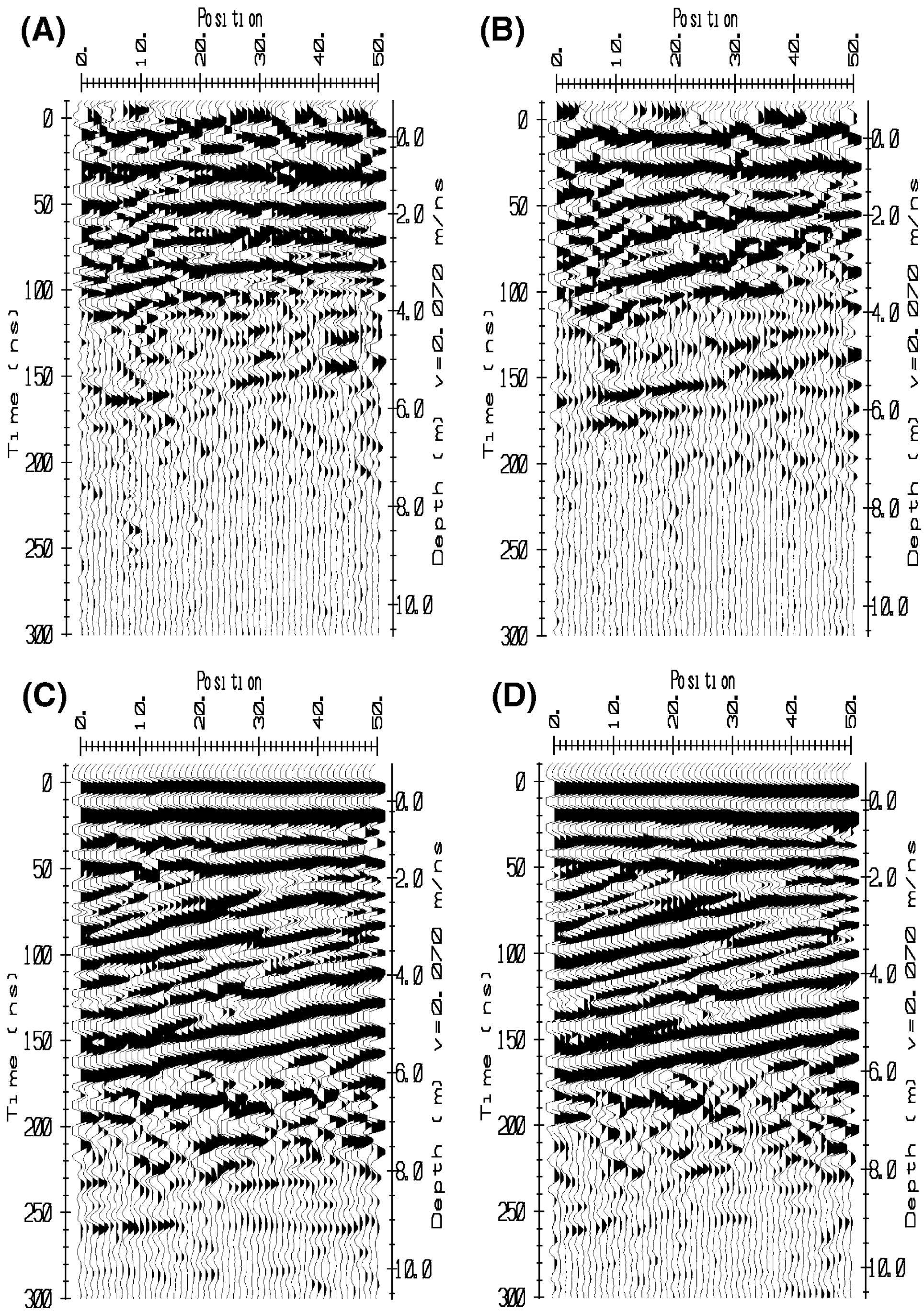

Fig. 8. Antennae orientation tests—along 75- to 125-m portion of the main test line. Antennae frequency 100 MHz with 1000 V transmitter pulser voltage (*x*-axis—distance in meters, 1-m trace interval; T—Transmitter, R—Receiver). (A) Cross-polarization—transmitter perpendicular, receiver parallel; (B) cross-polarization—transmitter parallel, receiver perpendicular; (C) parallel broadside; (D) perpendicular broadside.

reveal that both a decrease in antennae frequency and an increase in transmitter power resulted in an increase in depth of penetration and continuity of reflections, whereas an increase in antennae frequency for the same transmitter power showed an increase in resolution (Figs. 5 and 6). For the study site, optimum results in our opinion (comparison between resolution and depth of penetration) were obtained using 100-MHz antennae and a 1000-V transmitter. The 200-MHz antennae showed excellent resolution within the top 5–6 m but lacked penetration (Figs. 5D and 6C). The 25-and 50-MHz antennae showed deeper penetration (>10 m) than other frequencies but had reduced resolution (Figs. 5A,B and 6A). For this location, the 100-MHz antennae provided acceptable resolution, continuity of reflections, and penetrated to the base of the reflection pattern (deposit) being examined (7–8 m; Figs. 5C and 6B). Ideally, all antennae frequencies should be run at each site, but this would not be cost- and time-effective.

4.2. Crosslines

GPR profiles were run perpendicular (along strike) to the main test line, at the 50- and 100-m stations (Fig. 4), to examine facies and structure. The results for the 100-and 200-MHz antennae are shown in Fig. 7. The profiles show differences in resolution and depth of penetration: 7–8 m depth for 100-MHz and 5–6 m for 200-MHz antennae. They also show a different perspective in the depositional nature of the beach beds from the main test line. Strike profiles show horizontal to subhorizontal, nearly continuous bedding patterns in contrast to the inclined patterns in Figs. 5 and 6.

4.3. Antennae orientation

Annan (1992) demonstrated that there are various modes of antennae deployment. At the study site, four different antennae orientations were tested for their effectiveness in imaging sedimentary patterns along the main line from station 75 to 125 m (Fig. 4). A station interval of 1 m was used with the center of the antennae being 1 m apart. In Fig. 8A and B, are two different combinations of cross-polarization which show that the dipping reflections are chaotic in some locations. Fig. 8C shows data from a parallel broad-

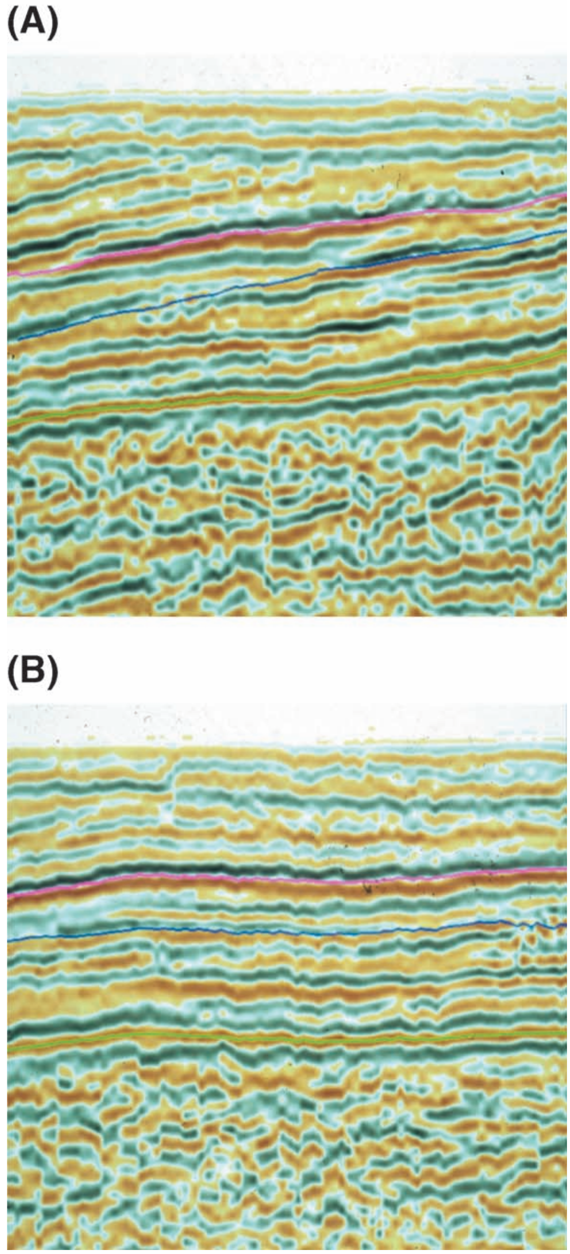

Fig. 9. Vertical sections (slices). The LANDMARK™ workstation allows one to pull GPR profiles from the test 3-D cube (see Fig. 4 for location) in a variety of directions; for example, (A) dip direction and (B) strike direction. These two profiles are similar to the GPR profiles presented in Figs. 5–7. The three-colored lines on (A) and (B) are picked events that will be used for demonstration purposes and each represents an upper shoreface/beachface.

side configuration, which is sometimes used in GPR surveying. The dipping stratigraphy is very apparent with good depth of penetration. The fourth test used the perpendicular broadside configuration (Fig. 8D), which is the most common survey procedure for both ease of data collection and accuracy of antennae placement. It also images the stratigraphy well with sufficient depth of penetration and is similar to, but not as deep as, results shown in Fig. 8C.

4.4. Grid pattern

Acquisition of radar profiles is nondestructive, quiet, relatively inexpensive, and rapid. However, similar to 2-D seismic reflection datasets, reflections and diffractions from structures off radar lines may cause ambiguities in the interpretation. The significantly greater reliability of 3-D seismic reflection data, demonstrated in numerous hydrocarbon exploration case histories (Brown, 1991), makes the adaptation of 3-D methods to radar studies an attractive proposition. The fundamental goal of geophysics for engineering and environmental applications is to reconstruct a 3-D map (or image) of the subsurface (Daniels et al., 1993). The recording, processing, and display of 3-D datasets have become a routine procedure in the seismic exploration industry (Brown, 1992), whereas it is only recently being used with GPR datasets (Daniels et al., 1993; Lawton et al., 1994; Ulriksen, 1994; Beres et al., 1995; Thompson et al., 1995; Jol et al., 1996c).

The objective of the grid survey at the test site was to evaluate the benefits of obtaining a 3-D data volume of GPR data for detailed stratigraphic mapping. GPR data were collected at 1-m intervals along parallel lines 50 m in length and spaced 1 m apart, yielding a 50 × 50 m grid (centered on the 100-m station of the original test line). The recording lines were oriented approximately in the direction of the stratigraphic dip. Data were collected with 100-MHz antennae and a 1000-V transmitter operated in a perpendicular broadside configu-

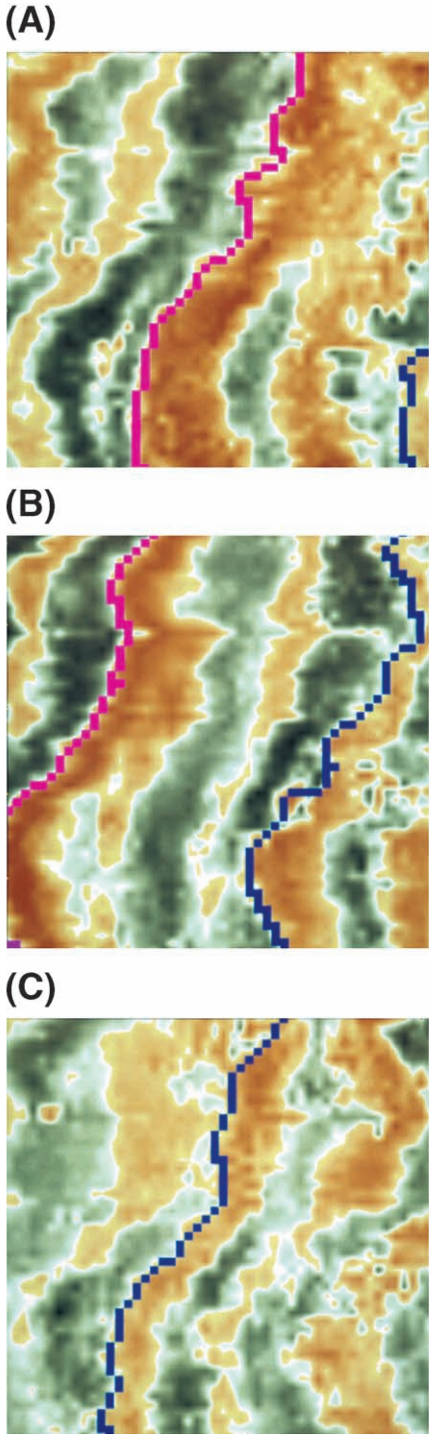

Fig. 10. Horizontal sections (known as time slices; north to the top) allow one to look down from above in a planform view and cut horizontal sections to see changes in stratigraphic patterns. (A) The upper horizontal section with the same interpreted events as Fig. 9. Lower horizontal sections (B and C, respectively) show that the picked events move down into the cube (dip) as well as move towards the northwest. The picked events also have a cuspate-like planform of the former beachfaces with a wavelength of ∼ 30 m.

ration with a separation of 1 m. High quality data, with events at up to 150 ns (depth of ~ 7 m), were obtained. After acquisition, data were converted to SEG-Y format, filtered to remove noise, and then entered into a LANDMARK™ seismic workstation for interpretation. The software enables the data to be displayed in a variety of orientations, including vertical sections in the dip direction (e.g., Fig. 9A) or in the strike direction (e.g., Fig. 9B) and horizontal sections called time slices (e.g., Fig. 10). Several events were mapped throughout the data volume, and these interpreted horizons were then extracted and displayed using 3-D rendering

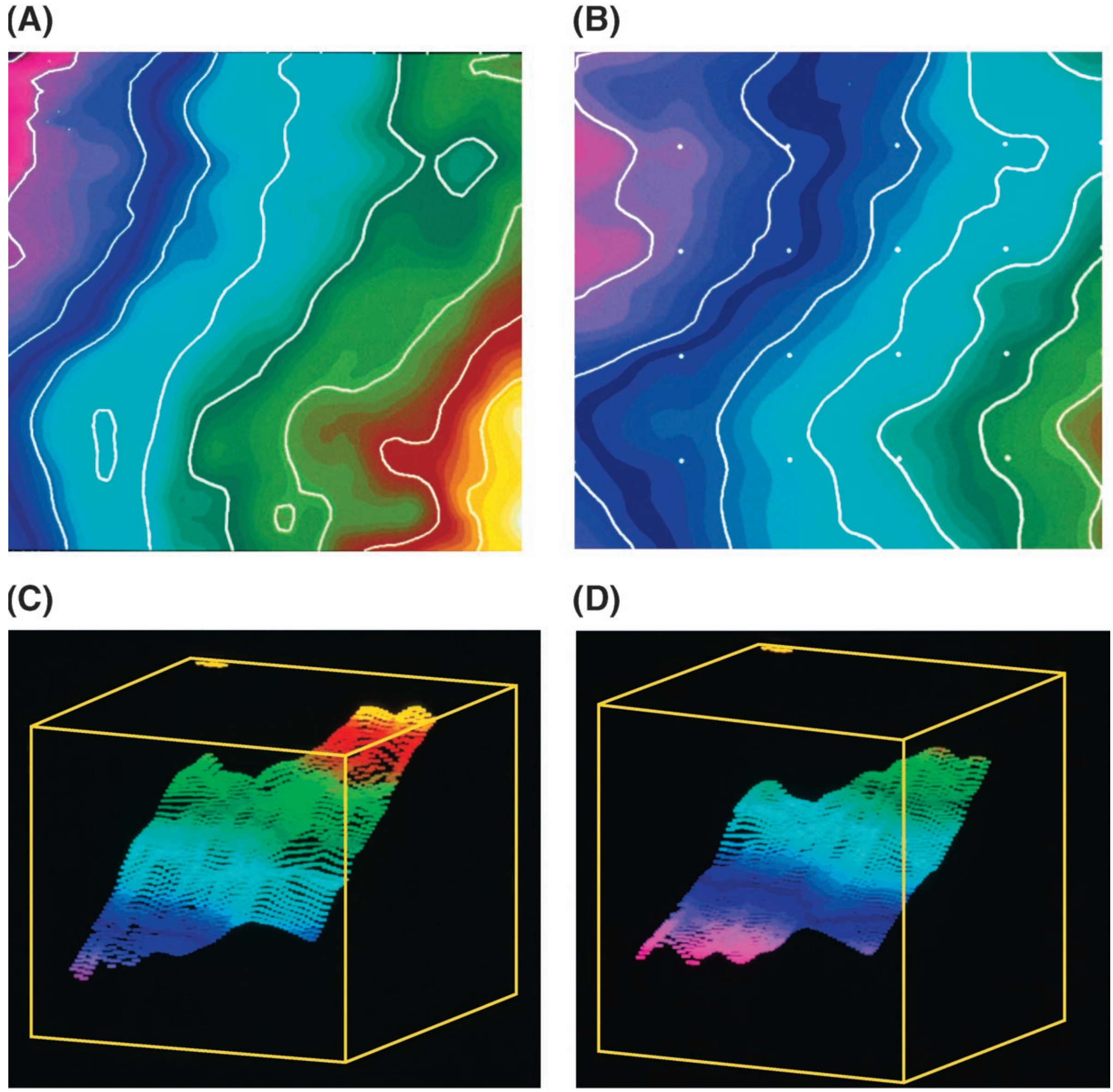

Fig. 11. Contour map and 3-D representation of individual picked events. Once an event is picked in LANDMARK™, these "layers" can be viewed as a contour plot (A and B; north to the top) or as a 3-D representation (C and D, north is to the left). The upper picked event (A and C) shows a steeper dipping beachface than the lower picked event (B and D). However, both events dip toward the northwest.

software. These images can be viewed from any perspective (e.g., Figs. 11 and 12); this greatly enhances one's ability to interpret the reflectivity fabric of the horizons and enables the 3-D depositional framework of the stratigraphic unit to be interpreted in more detail than that possible from widely spaced 2-D profiles. In the test volume, the processed GPR data cube shows a general shoreface dip ~ 1–2°, with slight long wavelength (~ 30 m) undulations in the strike direction.

Three-dimensional radar mapping has the potential to greatly improve our knowledge of distribution, geometries, and sediment facies of many high-energy depositional features. Huggenberger (1993) notes that this information could also be useful in the process of quantification of geophysical data as input for hydraulic conductivity models.

4.5. Geomorphic interpretation of the study site

GPR profiles at the test site indicate that the Willapa barrier spit has prograded seaward with the deposition of shingle-like accretionary layers. This result was not initially expected given the present

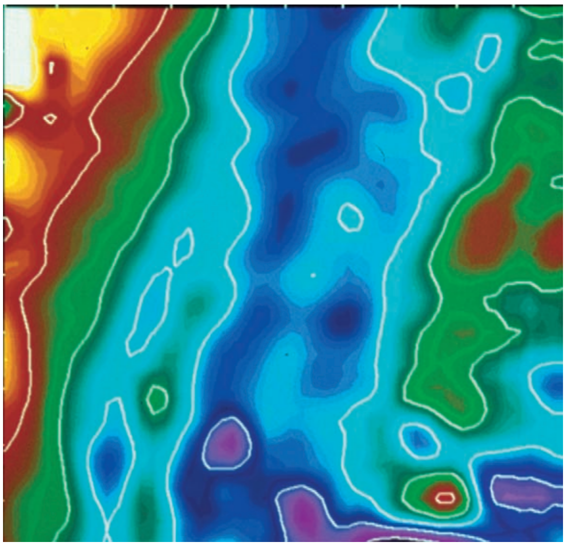

Fig. 12. Isopach map of sediment thickness (between middle and lower and picked events). Once events have been picked with LANDMARK™ software, the layers can be subtracted to get a thickness of sediment between two layers. This can aid in volume assessments as well as demonstrate where sediment accumulates. In this example of a prograding shoreline, most sediment has accumulated along the middle of the beachface with lower accumulation along the upper and lower portions of the beachface.

theory of barrier spit deposition in which progradation occurs in the direction of the dominant longshore transport (Nielsen et al., 1988). However, on the basis of radiocarbon dating, previous barrier research has also proposed a model of seaward migration by beach accretion (Bernard et al., 1962; Kraft, 1971; McCubbin, 1982). In this and other studies (Meyers et al., 1996; Smith et al., 1999), we have demonstrated a similar pattern through the interpretation of GPR data. The profiles and 3-D cube show that the upper 6–8 m of the barrier spit exhibit reflections dipping toward the ocean (west) at about 1–2°. These inclined, shingle-like reflections are interpreted as accretionary beachface/uppershore beds and are similar in appearance to the presently active beachface/upper shoreface environments. The layers also when mapped in 3-D also show undulations similar to the present beach. Such inclined strata are not normally detectable in trenches. Based on vibracoring, the portion of the profiles (below dipping reflections) where GPR reflections attenuate or become chaotic is the wave impact zone. This zone does not change significantly in grain size but is an area where the compactness (density) of the sediment increases (vibracoring becomes very difficult; Curt Peterson, Portland State University, personal communication, 2000). Signal loss as the result of salt water intrusion also occurs ~ 100 m landward of the high tide line.

5. Summary

Ground penetrating radar was used to examine the sedimentary structure and thickness of an active sandy barrier spit on the Pacific coast of Washington State, USA. GPR results provided high resolution (cm to m scale) continuous radar reflections that allowed for the determination of orientation, thickness, and style of major sedimentary structures and, therefore, sediment facies. Results from the test site enhance our ability to recognize major reflection patterns which will aid in understanding the complex subsurface architecture of coastal depositional environments. GPR can also be used to infer stratigraphic trends and, therefore, directions of progradation and/or aggradation.

The GPR tests indicated a 6- to 8-m-thick facies of shingle-like, accretionary beach beds and upper shoreface, which dip toward the ocean at ~ 1–2°. The strike profiles showed a horizontal to subhorizontal, nearly continuous reflection pattern. The loss of radar signal from below a depth of 6–8 m is the result of the wave impact zone (sediment compaction, change of lithofacies).

Different antennae frequencies and transmitter powers did provide alternative approaches to surveying study sites. In general, higher frequency antennae provided more vertical resolution, whereas lower frequencies provided greater depth of penetration and/or better continuity of reflections. Results from the present study demonstrated high resolution within the top 5–6 m with the 200-MHz antennae and deeper penetration (>10 m) with the 25- and 50-MHz antennae. For the study site, 100-MHz antennae provided a compromise between acceptable resolution and good continuity of reflections with a penetration depth of 7–8 m to the base of the dipping beach beds. Consequently, in areas where near subsurface detail is needed, 200-MHz antennae should be used. Where maximum depth of penetration is necessary, 25- or 50-MHz antennae should be used. Initial testing minimizes the time expended on a larger-scale survey and optimizes the quality of the data.

The parallel broadside and perpendicular broadside antennae orientation tests showed impressive stratigraphy, continuity of reflections, and depth of penetration, whereas the cross-polarization tests exhibited reduced continuity of reflections and less depth of penetration, but dipping reflections were apparent. Surprisingly, parallel broadside outperformed perpendicular broadside in terms of depth of penetration and continuity of reflections below a depth of 6 m.

The 3-D cube enables the 3-D subsurface geometry of the test site on the Willapa marine barrier system to be mapped. The 3-D depositional framework can be interpreted in more detail than possible from widely spaced 2-D profiles. This 3-D radar mapping has the potential to greatly improve our knowledge of the distribution and geometries of sediment facies in coastal environments and many other high-energy depositional geomorphic features.

Acknowledgements

Financial support for fieldwork was provided by grants from the Natural Sciences and Engineering Research Council of Canada (NSERC), Petrel-Robertson, Pan Canadian Petroleum, Amoco Canada, Canadian Hunter, Norcen Resources, The University of Calgary, University of Wisconsin-Eau Claire, and the U.S. Geological Survey. The authors wish to thank the community of Long Beach, the Cranberry Research Foundation, and the owners of the property where the study was conducted for their cooperation and helpfulness in the project. The CREWES Project at the University of Calgary is thanked for providing access to the LANDMARK™ workstation. Constructive reviews by J.R. Giardino and several anonymous reviewers are appreciated.

References

Annan, A.P., 1992. Ground Penetrating Radar Workshop Notes. Sensors and Software, Mississauga, ON.

Beres, M., Green, A., Huggenberger, P., Horstmeyer, H., 1995. Mapping the architecture of glaciofluvial sediments with three-dimensional georadar. Geology 23, 1087–1090.

Bernard, H.A., LeBlanc, R.J., Major, C.F., 1962. Recent and Pleistocene geology of southeast Texas. In: Rainwater, E.H., Zingula, R.P. (Eds.), Geology of the Gulf Coast and Central Texas, Guidebook of Excursions. Houston Geology Society, Houston, TX, USA, pp. 175–224.

Bristow, C.S., 1995. Internal geometry of ancient tidal bedforms revealed using ground penetrating radar. In: Flemming, B.W., Bartholoma, A. (Eds.), Tidal Signatures in Modern and Ancient Sediments. International Association of Sedimentologists, Special Publication, vol. 24, pp. 313–328. Oxford, UK.

Brown, A.R., 1991. Interpretation of 3-dimensional seismic data. Memoir - American Association of Petroleum Geologists, vol. 42. Tulsa, OK, 341 pp.

Brown, A.R., 1992. Seismic interpretation today and tomorrow. The Leading Edge 11 (11), 10–15.

Chiang, K.K., 1984. The giant Hoadley gas field, south-central Alberta. In: Masters, J.A. (Ed.), Elmworth-Case Study of a Deep Basin Gas Field. Memoir - American Association of Petroleum Geologists, vol. 38, pp. 297–313. Tulsa, OK.

Clifton, H.E., 1983. Discrimination between subtidal and intertidal facies in Pleistocene deposits, Willapa Bay, Washington. Journal of Sedimentary Petrology 53, 353–369.

Clifton, H.E., Phillips, R.L., 1980. Lateral trends and vertical sequences in estuarine sediments, Willapa Bay, Washington. In: Field, M.E., Bouma, A.H., Colburn, I.P., Douglas, R.G., Ingle, J.C. (Eds.), Quaternary Depositional Environments of the Pacific Coast. Pacific Coast Paleogeography Symposium, vol. 4. Pacific Section, Society of Economic Paleontologists and Mineralogists, Los Angeles, CA, pp. 55–71.

Daniels, D.J., Gunton, D.G., Scott, H.F., 1988. Introduction to subsurface radar. IEEE Proceedings 135 (Part F, No. 4), 277–305.

Daniels, J.J., Ansari, W., Grumman, D., Roberts, R., 1993. 3-D GPR.

Advanced Ground Penetrating Radar: Technologies and Applications. Proceedings, Second Gov. Workshop on GPR, The Ohio State University, October 26–28, Columbus, Ohio. Ohio State University, Columbus, OH, USA, pp. 307–318.

Davis, J.L., Annan, A.P., 1989. Ground penetrating radar for high resolution mapping of soil and rock stratigraphy. Geophysical Prospecting 37, 531–551.

Huggenberger, P., 1993. Radar facies: recognition of characteristic braided river structures of the Pleistocene Rhine gravel (NE part of Switzerland). In: Best, J., Bristow, C.S. (Eds.), Braided Rivers. Geological Society Special Publication, vol. 75, pp. 163–175. London, UK.

Jol, H.M., 1995. Ground penetrating radar antennae frequencies and transmitter powers compared for penetration depth, resolution and reflection continuity. Exploration Geophysics 43, 693–709.

Jol, H.M., Smith, D.G., 1991. Ground penetrating radar of northern lacustrine deltas. Canadian Journal of Earth Sciences 28, 1939–1947.

Jol, H.M., Smith, D.G., Meyers, R.A., Lawton, D.C., 1996a. Ground penetrating radar: high resolution stratigraphic analysis of coastal and fluvial environments. In: Pacht, J.A., Sheriff, R.E., Perkins, B.F. (Eds.), Stratigraphic Analysis Using Advanced Geophysical, Wireline and Borehole Technology for Petroleum Exploration and Production. Gulf Coast Section, Society of Economic Paleontologists and Mineralogists Foundation, 17th Annual Research Conference, Houston, TX. Gulf Coast Section SEPM Foundation, Houston, TX, USA, pp. 153–163.

Jol, H.M., Smith, D.G., Meyers, R.A., 1996b. Digital ground penetrating radar (GPR): an improved and very effective geophysical tool for studying modern coastal barriers (examples for the Atlantic, Gulf and Pacific coasts, U.S.A.). Journal of Coastal Research 12 (4), 960–968.

Jol, H.M., Smith, D.G., Meyers, R.A., 1996c. Three dimensional GPR imaging of a fan-foreset delta: an example from Brigham City Utah, U.S.A. Proceedings of the Sixth International Conference on Ground Penetrating Radar (GPR '96), September 30–October 3, Sendai, Japan. Tohoku University, Sendai, Japan, pp. 33–37.

Kaminsky, G.M., Buijsman, M., Gelfenbaum, G.R., Ruggiero, P., Jol, H.M., Gibbs, A., Peterson, C.D., 1999. Synthesizing geological observations and process-response data for modeling coastal change at a management scale. Proceedings of Coastal Sediments '99. ASCE, Long Island, NY, pp. 1708–1723.

Kraft, J.C., 1971. Sedimentary facies patterns and geologic history of a Holocene marine transgression. Geological Society of America Bulletin 82, 2131–2158.

Lawton, D.C., Jol, H.M., Meyers, R.A., 1994. 3-D ground penetrating radar surveys: a new approach to imaging and visualising the near surface. Abstracts for Poster Papers, Fifth Int. Conf. on GPR, June 12–16, Kitchener, Ontario, Canada. University of Waterloo, Waterloo, ON, Canada, p. 16.

Leatherman, S.P., 1987. Coastal geomorphic applications of ground penetrating radar. Journal of Coastal Research 3 (3), 397–399.

McCubbin, D.G., 1982. Barrier-island and strand-plain facies. In: Scholle, P.A., Spearing, D. (Eds.), Sandstone Depositional Environments. Memoir - American Association of Petroleum Geologists, vol. 31, pp. 247–279. Tulsa, OK.

Meyers, R.A., 1994. The Willapa barrier spit of S.W. Washington State: depositional processes inferred from ground penetrating radar. MS Thesis. University of Calgary, Alberta, Canada. 101 pp.

Meyers, R.A., Smith, D.G., Jol, H.M., Peterson, C.R., 1996. Evidence for eight great earthquake subsidence events detected with ground-penetrating radar, Willapa barrier, Washington. Geology 24, 99–102.

Neal, A., Roberts, C.L., 2000. Applications of ground penetrating radar (GPR) to sedimentological, geomorphological and geoarchaeological studies in coastal environments. In: Pye, K., Allen, J.R.L. (Eds.), Coastal and Estuarine Environments: Sedimentology, Geomorphology and Geoarchaeology. Geological Society, Special Publications, vol. 175, pp. 139–171. London, UK.

Nielsen, L.H., Johannessen, P.N., Surlyk, F., 1988. A Late Pleistocene coarse-grained spit–platform sequence in northern Jylland, Denmark. Sedimentology 35, 915–937.

Reinson, G.E., 1984. Barrier-islands and associated strand-plain systems. In: Walker, R.G. (Ed.), Facies Models. Geological Association of Canada Reprint Series, vol. 1, pp. 119–140. Toronto, ON.

Smith, D.G., Jol, H.M., 1995. Ground penetrating radar: antennae frequencies and maximum probable depths in Quaternary sediments. Journal of Applied Geophysics 33, 93–100.

Smith, D.G., Zorn, C.E., Sneider, R.M., 1984. Paleogeography of the lower Cretaceous of western Alberta and northeastern British Columbia in and adjacent to the deep basin of the Elmworth area. In: Master, J.A. (Ed.), Elmworth-Case Study of a Deep Basin Gas Field. Memoir - American Association of Petroleum Geologists, vol. 38, pp. 79–114. Tulsa, OK.

Smith, D.G., Meyers, R.A., Jol, H.M., 1999. Sedimentology of an upper-mesotidal (3.7 m) Holocene barrier, Willapa Bay, SW Washington, U.S.A. Journal of Sedimentary Research 69, 1290–1296.

Thompson, C., McMechan, G., Szerbiak, R., Gaynor, N., 1995. Three-dimensional GPR imaging of complex stratigraphy within the Ferron sandstone, Castle Valley, Utah. Symposium on the Application of Geophysics to Engineering and Environmental Problems Proceedings Orlando, FL. Environmental and Engineering Geophysical Society, Wheat Ridge, CO, USA, pp. 435–443.

Ulriksen, C.P.F., 1982. Application of impulse radar to civil engineering. PhD dissertation. Lund University of Technology, Lund, Sweden. 175 pp.

Ulriksen, C.P.F., 1994. Assessment of infrastructure and environmental conditions using GPR. Introduction to Applied Geophysics: Short Course, Sym. on the Application of Geophysics on Engineering and Environmental Problems (SAGEEP), Section 1, March 27, Boston, MA.

Van Heteren, S., Fitzgerald, D.M., Barber, D.C., Kelley, J.T., Belknap, D.F., 1996. Volumetric analysis of a New England barrier system using ground-penetrating-radar and coring techniques. Journal of Geology 104, 471–483.

Van Heteren, S., Fitzgerald, D.M., McKinlay, P.A., Buynevich, I.V., 1998. Radar facies of paraglacial barrier systems: coastal New England, USA. Sedimentology 45, 181–200.